Arch. Mech., 49, 1, pp. 111–127, Warszawa 1997

Unsteady compressible boundary layer flow at the stagnation point of a rotating sphere with an applied magnetic field

A. SAU and G. NATH (BANGALORE)

THE PAPER is concerned with the unsteady compressible boundary layer flow near the forward stagnation point of a rotating sphere in a uniform axial stream of conducting fluid, with magnetic field normal to the surface. The unsteadiness in the flow is created by (i) giving a sudden change in the wall temperature (enthalpy) as the impulsive motion has started, (ii) impulsive change of the rotation of the sphere, and (iii) sudden changing of the free stream velocity. The motion is governed by a coupled set of three nonlinear time-dependent partial differential equations which are solved accurately by Newton's linearization technique and an implicit finite difference scheme. Attention is given to the transient phenomenon from the initial flow to the final steady state solution. The numerical results show changes in the flow pattern with time, rotation and strength of the magnetic field, and are in good agreement with earlier theoretical results. The calculated skin friction, heat transfer, displacement thickness and enthalpy thickness show interesting dependence on time and the physical parameters, which are quite similar to the earlier investigations, and the mechanism of dependence is closely examined.

1. Introduction

CURRENT USE of blunt bodies of revolution for the solution of hypersonic flight problems has placed special emphasis on accurate prediction of aerodynamic heating. Design of hypersonic re-entry vehicles such as a re-entering satellite requires reasonably accurate predictions of the stagnation point heat transfer to obtain optimum configurations. The high stagnation temperature accompanying flight at high Mach numbers renders the air sufficiently ionized behind the bow shock so that it may be considered as an electrically conducting fluid. Under these circumstances, the presence of a magnetic field will tend to modify both the flow field and the heat transfer.

An axisymmetric boundary layer flow over a rotational symmetric body set into impulsive axial motion was first studied by BOLTZE [1], who expanded the stream function and vorticity in series of powers of time (t) after the impulsive start and obtained numerical solution for terms up to t^3. DENNIS and WALKER [2] improved the accuracy of Boltze solution by numerically computing the solution for terms up to t^7. The unsteady flow past an impulsively started sphere has also been discussed by DENNIS and WALKER [3] and the results were extended to larger values of time. The boundary layer growth near the equator of an impulsively started sphere was considered by BANKS and ZATUSKA [4]. The evolution of unsteady boundary layers close to the stagnation region of a slender prolate spheroid in uniform motion at constant angle of attack after an impulsive start have been discussed by CEBECI *et al.* [5]. DENNIS and DUCK [6] have presented the Navier-Stokes solutions for an impulsively started rotating sphere. In a recent study DUCK [7] investigated the effect of small amplitude, time-periodic, free stream disturbances on the axisymmetric boundary layers. The unsteady boundary layer flow past an impulsively started translating and spinning, rotationaly symmetric body has been studied by ECE [8], and he obtained initial stages of flow by expanding the stream function and swirl velocity in series of power of time. All the above studies deal with incompressible flows. KUMARI and NATH [9] have studied the unsteady compressible stagnation point boundary layer flow over a rotating body of revolution (sphere) when the free stream velocity, rotation, the surface mass transfer and the wall temperature varied arbitrarily with time. VIMALA and NATH [10] have solved the two-dimensional stagnation point flow for accelerating and oscillating free streams.

In this paper we evaluate the characteristics of unsteady compressible boundary layer flow of an electrically conducting fluid near the forward stagnation point of a rotating sphere, immersed in a uniform flow and having a normal magnetic field applied at the surface. Three separate situations have been considered in which there is an initial steady state that is perturbed by either (i) a step change in the wall enthalpy, (ii) a sudden change in the rotational velocity, and (iii) a sudden change in mainstream speed. The time-dependent development of the boundary layer is computed until a new steady state is reached. Extensive numerical results are presented showing the temporal development of various boundary layer properties.

2. Basic equations and boundary conditions

To fix the problem mathematically, we consider an orthogonal curvilinear coordinate system (Fig. 1) in which x measures the distance along a meridian from the forward stagnation point, y represents the distance in the direction of rotation, and z its distance normal to the body. We assume the flow to be axisymmetric and the external flow is homentropic, the dissipation terms and effect of surface curvature being negligible near the stagnation point; $r(x)$, the normal distance of a point on the body from the axis of rotation is equal to x in the neighbourhood of the pole (or stagnation point in this case). A uniform magnetic field of strength B_0 is applied to the boundary layer in the z-direction. The magnetic Reynolds number is considered to be small, hence the magnetic field becomes independent of fluid motion. At time $t \leq 0$, the total enthalpy at the wall is H_w, and at $t > 0$ it is impulsively changed to H_w^*. Alternatively, at time $t \leq 0$, the angular velocity of rotation is Ω, and at $t > 0$ it is impulsively changed to Ω^*. Similarly at $t \leq 0$, the meridional component of free-stream velocity is u_e, and at time $t > 0$ it is suddenly changed to u_e^*. These sudden changes cause unsteadiness in the flow field. Under the foregoing assumptions, the boundary layer equations for the unsteady

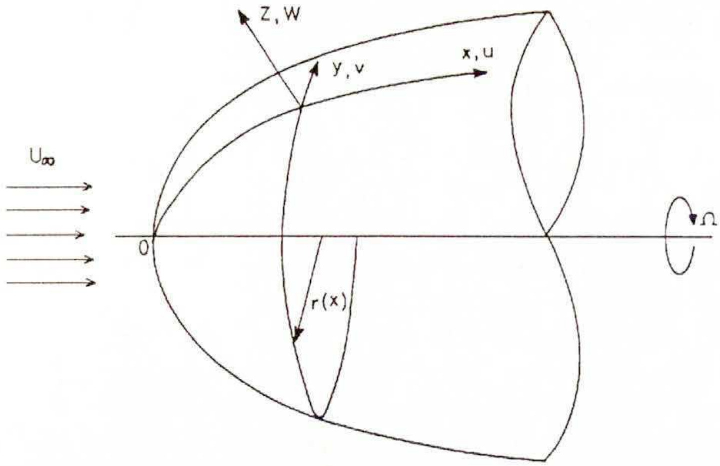

FIG. 1. Flow model and coordinate system for a rotating body of revolution.

compressible flow are given by [11, 12]

$$(\varrho x)_t + (\varrho x u)_x + (\varrho x w)_z = 0, \tag{2.1}$$

$$\begin{aligned} &\varrho(u_t + uu_x + wu_z - v^2/x) \\ &\qquad = \varrho_e\left[(u_e)_t + u_e(u_e)_x\right] + (\mu u_z)_z - B_0^2(\sigma u - \sigma_e u_e), \\ &\varrho(v_t + uv_x + wv_z + uv/x) = (\mu v_z)_z - \sigma B_0^2 v, \\ &\varrho(H_t + uH_x + wH_z) = \left(\frac{\mu}{\mathrm{Pr}} H_z\right)_z, \end{aligned} \tag{2.2}$$

where u, v, w are the velocity components along the x, y, z axes, respectively. ϱ, μ, σ and Pr are, respectively, the density, viscosity, electrical conductivity and the Prandtl number; H is the total enthalpy and u_e is the x-component of the flow velocity at the edge of the boundary layer. The subscripts denote the partial derivatives with respect to the corresponding variables.

The initial and boundary conditions are:

$$\begin{aligned} &\text{at } t = 0: \\ &\qquad u(x,0,z) = u_i(x,z), \qquad v(x,0,z) = v_i(x,z), \\ &\qquad w(x,0,z) = w_i(x,z), \qquad H(x,0,z) = H_i(x,z), \\ &\text{and for } t > 0: \\ &\qquad u(x,t,0) = 0, \qquad v(x,t,0) = \Omega^* x, \\ &\qquad w(x,t,0) = w_w, \qquad H(x,t,0) = H_w^*, \\ &\qquad u(x,t,\infty) = u_e^*(x,t), \qquad v(x,t,\infty) = 0, \\ &\qquad H(x,t,\infty) = H_e\,. \end{aligned} \tag{2.3}$$

The subscripts i, w, e denote initial conditions, conditions at the wall and at the edge of the boundary layer, respectively.

3. Boundary layer transformations

Now we introduce the transformations

$$\eta = \left(\frac{2a\varrho_e}{\mu_e}\right)^{1/2} \int\limits_0^z \frac{\varrho}{\varrho_e} dz, \qquad t^* = at,$$

a is a constant having dimension (time)$^{-1}$,

$$u = u_e F(\eta, t^*), \qquad F = f', \qquad u_e = ax,$$

$$v = v_w s(\eta, t^*), \qquad v_w = \Omega x, \qquad H = H_e g(\eta, t^*).$$

We assume that the fluid has variable properties $\varrho \propto T^{-1}$, $\mu \propto T^{\omega}$, $\sigma \propto T^n$, where T is the temperature, $0 < \omega \leq 1$ is the index in the power-law variation of viscosity and n is the exponent in the power-law variation of electrical conductivity of the fluid. The set of Eqs. (2.2), with the help of continuity Eq. (2.1) and the above transformations, reduce, respectively, to

$$\begin{aligned} (NF')' + fF' + (g - F^2)/2 + \lambda^2 s^2/2 - Mg(Fg^n - 1)/2 - F_{t^*}/2 &= 0, \\ (Ns')' + fs' - Fs - Msg^{n+1}/2 - s_{t^*}/2 &= 0, \\ (Ng')' + \Pr fg' - \Pr g_{t^*}/2 &= 0, \end{aligned} \tag{3.1}$$

where F, s and g are non-dimensional meridional and azimuthal velocity and non-dimensional total enthalpy, respectively. The prime and the subscript t^* denote the partial differentiation with respect to the variables η and t^*, respectively.

Use is made of the following relations:

$$\varrho_e/\varrho = T/T_e = h/h_e = H/H_e = g$$

(since $h/h_e \to H/H_e$ at the stagnation region, h being the specific enthalpy),

$$N = \varrho\mu/\varrho_e\mu_e = (T/T_e)^{\omega-1} = g^{\omega-1}, \qquad \sigma = \sigma_e(T/T_e)^n = \sigma_e g^n,$$

$\lambda = \Omega/a$ is the rotation parameter,

$$M = \frac{\text{ponderomotive force}}{\text{inertia force}} = \frac{\sigma_e B_0^2 x}{\varrho_e u_e}.$$

The initial conditions are governed by the solution of the corresponding steady state equations obtained from Eqs. (3.1) by putting $F_{t^*} = s_{t^*} = g_{t^*} = 0$ in them. As stated earlier, there will be three different cases under the present study and the relevant boundary conditions corresponding to each case are:

CASE 1. At time $t^* \leq 0$, let the wall enthalpy be H_w (constant), and at time $t^* > 0$, there is a sudden change Δ_1 in the wall enthalpy and it is then maintained for subsequent time (i.e., for $t^* > 0$, $H_w^* = H_w(1 + \Delta_1)$), whereas free stream velocity in x-direction u_e and the angular velocity of rotation Ω remain the same for all time. In such a case, the boundary conditions in non-dimensional form reduce to:

$$
\begin{aligned}
&\text{for } t^* > 0, \\
&\qquad f = f_w, \qquad F = 0, \qquad s = 1, \\
&\qquad g = g_w + \Delta, \qquad (\Delta = \Delta_1 g_w) \qquad \text{at } \eta = 0, \\
&\qquad F = 1, \qquad s = 0, \\
&\qquad g = 1 \qquad \text{as } \eta \to \infty, \\
&\text{and at } t^* = 0, \\
&\qquad \Delta = 0.
\end{aligned}
\tag{3.2}
$$

CASE 2. In this case, instead of changing the wall enthalpy, a sudden change ($\Omega^* = \Omega(1+\Delta)$, $\Delta = 0$ for $t^* \leq 0$ and $\Delta = \text{const}$ for $t^* > 0$) in the angular velocity of rotation is considered, so that the boundary conditions in non-dimensional form become:

$$
\begin{aligned}
&\text{for } t^* > 0, \\
&\qquad f = f_w, \qquad F = 0, \\
&\qquad s = 1 + \Delta, \qquad g = g_w \qquad \text{at } \eta = 0, \\
&\qquad F = 1, \qquad s = 0, \\
&\qquad g = 1 \qquad \text{as } \eta \to \infty, \\
&\text{and at } t^* = 0, \\
&\qquad \Delta = 0.
\end{aligned}
\tag{3.3}
$$

CASE 3. An impulsive change in the free-stream velocity in meridional direction is considered in this case. For time $t^* \leq 0$, let the velocity be u_e and at time $t^* = 0$, an impulsive change $u_e^* = u_e(1 + \Delta)$ to the free stream velocity is given and kept steady thereafter. So the boundary conditions in non-dimensional form reduce to:

$$
\begin{aligned}
&\text{for } t^* > 0, \\
&\qquad f = f_w, \qquad F = 0, \\
&\qquad s = 1, \qquad g = g_w \qquad \text{at } \eta = 0, \\
&\qquad F = 1 + \Delta, \qquad s = 0, \\
&\qquad g = 1 \qquad \text{as } \eta \to \infty, \\
&\text{and at } t^* = 0, \\
&\qquad \Delta = 0,
\end{aligned}
\tag{3.4}
$$

where

$$
f = \int_0^\eta F\, d\eta + f_w \qquad \text{and} \qquad f_w = -(\varrho w)_w (\mathrm{Re}_x/2)^{1/2} / \varrho_e u_e
$$

is constant under the assumption that $(\varrho w)_w$ is constant. The parameter f_w is called the mass transfer parameter and it corresponds to suction or injection, according to whether $f_w > 0$ or $f_w < 0$ and $\mathrm{Re}_x = u_e x/\nu_e$ is the local Reynolds number.

4. Results and discussions

The time-dependent boundary layer Eqs. (3.1) subject to the boundary conditions (3.2) or (3.3) or (3.4) which correspond to the different types of flow situations considered and the initial conditions have been solved numerically using Newton's linearization method and an implicit finite difference scheme of the Crank–Nicolson type. The grid sizes that we have used are as follows: $\delta t^* = 0.00025$ for $t^* \le 0.05$, $\delta t^* = 0.001$ for $0.05 < t^* \le 0.1$, $\delta t^* = 0.005$ for $0.1 < t^* \le 0.5$, $\delta t^* = 0.01$ for $t^* > 0.5$, and $\delta\eta = 0.01$ is kept fixed throughout the computation. The choice of grid lengths has been found to be optimum since further reduction does not affect the results at least up to the fourth decimal place. The selection of $\delta\eta$ is made such that it does not affect the results, even when $\eta = O((t^*)^{1/2})$ and t^* is small. The solutions were iterated until the convergence criterion based on the wall shear and the heat transfer parameters F'_w, s'_w, g'_w is satisfied, that is

$$\text{Maximum}\left[\left|(F'_w)^{n+1} - (F'_w)^n\right|, \left|(s'_w)^{n+1} - (s'_w)^n\right|, \left|(g'_w)^{n+1} - (g'_w)^n\right|\right] < \delta_1 ,$$

where δ_1 is a tolerance parameter which was set equal to 10^{-4} in the calculations.

The quantities of physical interest are the skin friction and heat transfer coefficients, displacement and enthalpy thicknesses. Based on u-velocity, the equation defining the skin friction coefficient is

$$C_{f_x} = \frac{2\left(\mu \dfrac{\partial u}{\partial z}\right)_{\eta=0}}{\varrho_e \left(u_e^2\right)_{t^*=0}} = 2^{3/2}\mathrm{Re}_x^{-1/2} N_w F'_w = 2^{3/2}\mathrm{Re}_x^{-1/2}\overline{C}_{f_x} ,$$

where $\overline{C}_{f_x} = N_w F'_w$.

Displacement and enthalpy thicknesses based on u-velocity are defined as [11]

$$\delta_x^* = \int_0^\infty [1 - \varrho u/\varrho_e u_e]\, dz = x(2\mathrm{Re}_x)^{-1/2} \int_0^\infty (g - F)\, d\eta = x(2\mathrm{Re}_x)^{-1/2}\overline{\delta}_x^*,$$

$$\overline{\delta}_x^* = \delta_x^*(2\mathrm{Re}_x)^{1/2}/x;$$

$$\delta_{H_x} = \int_0^\infty \frac{\varrho u}{\varrho_e \mu_e}\left[\frac{h}{h_e} - 1\right] dz = x(2\mathrm{Re}_x)^{-1/2}\int_0^\infty F(g-1)\, d\eta = x(2\mathrm{Re}_x)^{-1/2}\overline{\delta}_{H_x},$$

$$\overline{\delta}_{H_x} = \delta_{H_x}(2\mathrm{Re}_x)^{1/2}/x.$$

Analogously, we define the quantities based on v-profiles;

$$C_{f_y} = \frac{2\left(\mu \dfrac{\partial v}{\partial z}\right)_{\eta=0}}{\varrho_e \left(u_e^2\right)_{t^*=0}} = 2^{3/2}\mathrm{Re}_x^{-1/2}\lambda N_w s'_w = 2^{3/2}\mathrm{Re}_x^{-1/2}\overline{C}_{f_y},$$

where $\overline{C}_{f_y} = \lambda N_w s'_w$,

$$\delta_y^* = \int_0^\infty \frac{\varrho v}{\varrho_w v_w} dz = x(2\mathrm{Re}_x)^{-1/2}\int_0^\infty g_w s\, d\eta,$$

$$\delta_{H_y} = \int_0^\infty \frac{\varrho v}{\varrho_w v_w}\left[\frac{h}{h_e} - 1\right] dz = x(2\mathrm{Re}_x)^{-1/2}\int_0^\infty s g_w (g-1)\, d\eta.$$

However, in the present study only δ_x^* and δ_{H_x} will be presented.

The heat transfer coefficient in terms of the Stanton number is

$$\mathrm{St} = \frac{\left(\dfrac{\mu}{\mathrm{Pr}}\dfrac{\partial H}{\partial z}\right)_{\eta=0}}{(H_e - H_w)\varrho_e (u_e)_{t^*=0}} = \mathrm{Pr}^{-1}(\mathrm{Re}_x/2)^{-1/2} N_w g'_w/(1-g_w) = (\mathrm{Re}_x/2)^{-1/2}\overline{\mathrm{St}},$$

where

$$\overline{\mathrm{St}} = \mathrm{Pr}^{-1} N_w g'_w/(1-g_w).$$

F'_w and s'_w are called skin friction parameters in the respective directions and g'_w is the heat transfer parameter.

Table 1. Comparison of skin friction and heat transfer parameters (F'_w, g'_w) with BADE [13] for Pr = 2/3, $f_w = 0.0$, $\lambda = 0$ and $M = 0$.

ω	g_w	F'_w		g'_w	
		Present study	BADE [13]	Present study	BADE [13]
1.0	0.2	0.6304	0.6303	0.3437	0.3438
1.0	0.8	0.8565	0.8566	0.0910	0.0909
0.7	0.4	0.5838	0.5837	0.2125	0.2125
0.7	0.8	0.8203	0.8202	0.0866	0.0865
0.5	0.2	0.3445	0.3447	0.1797	0.1796
0.5	0.4	0.5139	0.5137	0.1846	0.1845

Computations have been carried out on a CYBER-992 computer for various values of f_w ($-0.5 \le f_w \le 0.5$), λ ($2 \le \lambda \le 10$), M ($5 \le M \le 10$), ω ($0.5 \le \omega \le 1.0$) and g_w ($0.6 \le g_w \le 2.2$). For all the results which we present here we have assumed the Prandtl number Pr = 0.72 and $n = 1.5$. In order to accommodate the rapid thickening of boundary layer as the impulsive motion has started, we have taken the far field conditions at $\eta = \eta_\infty = 20$. At this point we should mention that our steady equations for a stationary sphere and without magnetic field coincides with those of VIMALA and NATH [10], when we replace a by $a/2$ in the definition of η. A table of comparison (Table 1) and Fig. 2 show encouraging agreement with previous theories [10, 13] for some special cases. Moreover, our steady results for uniform rotation show excellent agreement with Ref. [9], but the comparison is not shown here for the sake of brevity.

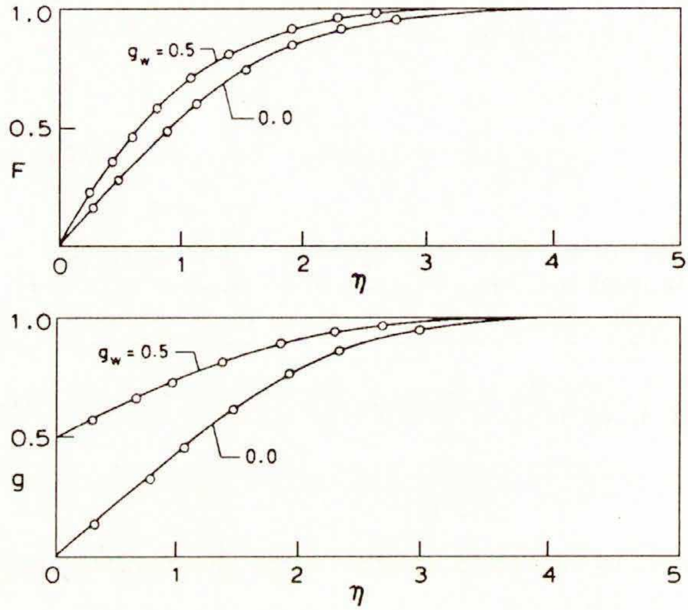

FIG. 2. Comparison of velocity (F) and enthalpy (g) profiles with the results of VIMALA and NATH [10] for $t^* = 0$, Pr = 0.72, $\omega = 1$, $f_w = 0$, $\lambda = 0$, $M = 0$; ○ results due to Ref. [10]; —— present study.

CASE 1. Unsteadiness caused by sudden change in wall enthalpy

The sphere is assumed to be rotating with constant angular velocity in a uniform stream of conducting fluid. A forced convection thermal boundary layer is then produced by impulsive changing of the wall temperature (enthalpy) of the sphere which was initially kept at a temperature (enthalpy) higher than the surrounding fluid temperature (enthalpy).

Figure 3 shows the effects of rotation (λ) and magnetic parameter (M) on the skin friction and heat transfer coefficients ($\overline{C}_{f_x}, -\overline{C}_{f_y}, \overline{\mathrm{St}}$) and their variation with time when the wall enthalpy is changed impulsively. The results show that both meridional skin friction and heat transfer [$\overline{C}_{f_x}, \overline{\mathrm{St}}$] increase (decrease) suddenly to a maximum (minimum) value from their initial steady state (depending on the impulsive increase or decrease in the wall enthalpy), as the impulse is given at time $t^* > 0$. And then the quantities steadily decrease (increase) with time, finally

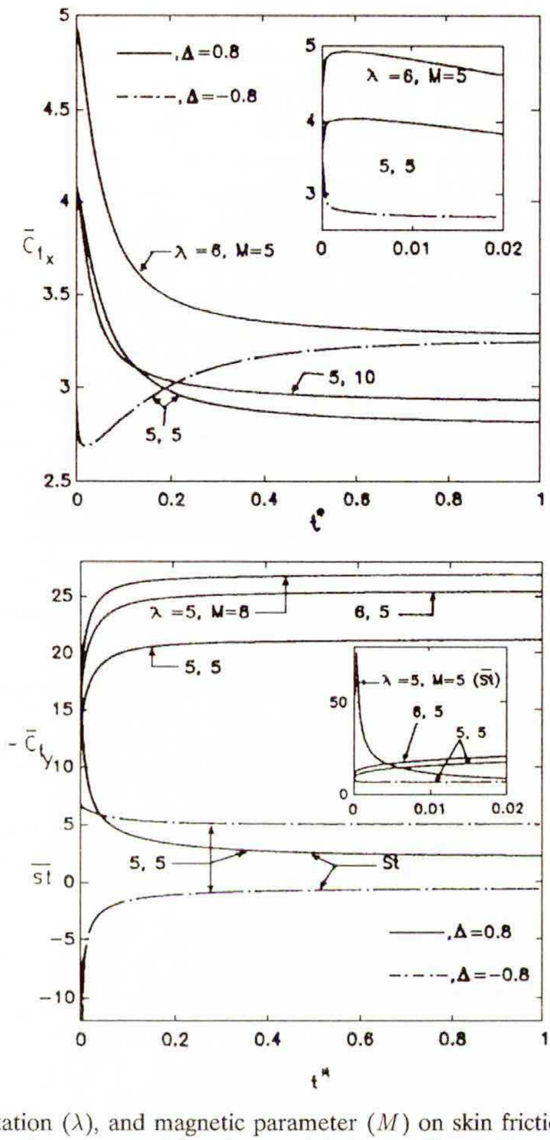

FIG. 3. Effects of rotation (λ), and magnetic parameter (M) on skin frictions and heat transfer ($\overline{C}_{f_x}, -\overline{C}_{f_y}, \overline{\mathrm{St}}$) for $f_w = 0$, $\omega = 0.5$ and $g_w = 1.4$; (unsteadiness due to impulsive change in wall enthalpy).

asymptotically approaching a clearly defined new steady state. From the inset of Fig. 3 (showing the behaviour of the physical quantities at time $t^* = 0+$) we see that mostly heat transfer suffers sudden change immediately after the impulse, whereas azimuthal skin friction $[-\overline{C}_{f_y}]$ shows its smooth transition. Moreover, it is observed that the skin frictions reach their steady state faster than the heat transfer. This is due to the fact that we have considered the case of impulsive wall heating (cooling), which also causes a rapid change in the heat transfer at the wall near $t^* = 0$. As rotation (λ) increases, both skin friction and heat transfer increase (however, its effect on the heat transfer is not shown here for the sake of compactness), and the effect is more pronounced on the azimuthal skin friction [$\overline{C}_{f_y}$]. This is because the shear force between the sphere and the adjacent fluid layer increases for higher rotation and its component in the azimuthal direction dominates for the simple reason that the direction of rotation of the sphere coincides with the azimuthal direction. But the basic trend of the flow behaviour immediately after the impulse remains the same for higher rotation. Figure 3 also shows that an increase in magnetic field strength (M) causes skin frictions to increase, whereas its effect is observed to be negligible on the heat transfer. Another phenomenon may be observed that an impulsive increase and an impulsive decrease of wall enthalpy by the same amount does not reflect its effect on the physical quantities as mirror images. It can be seen more clearly in the subsequent figures that the impulsive decreasing processes take more time to reach a new steady state compared to the impulsive increasing processes.

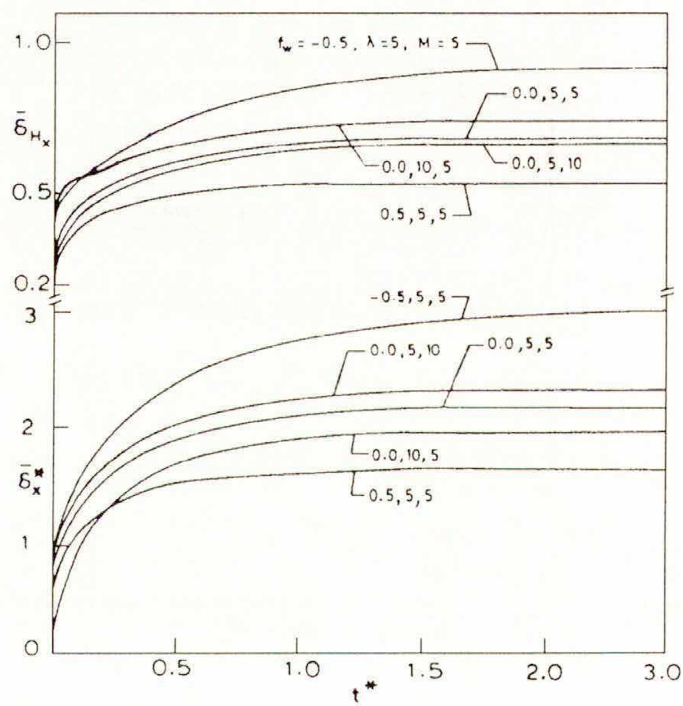

FIG. 4. Effects of mass transfer (f_w), rotation (λ), and magnetic parameter (M) on displacement and enthalpy thickness [$\overline{\delta}^*_x, \overline{\delta}_{H_x}$] for $\Delta = 0.8$, $\omega = 0.5$ and $g_w = 1.4$; (unsteadiness due to impulsive increase in wall enthalpy).

Figure 4 shows the effects of mass transfer (f_w), rotation (λ) and the magnetic parameter (M) on displacement thickness ($\overline{\delta}^*_x$) and enthalpy thickness ($\overline{\delta}_{H_x}$) when an impulsive increase in the wall enthalpy is considered. Both the displacement and enthalpy thickness are found to increase with time and they reach a steady state value for $t^* \geq 3$, and do not show any singular behaviour. With injection ($f_w < 0$), both displacement and entalphy thickness are found to increase but they show reverse effect with suction ($f_w > 0$). This is due to the fact that the injected coolant pushes the boundary layer away from the surface and establishes a heat insulating layer, whereas suction works in the reverse way. As rotation (λ) increases, the displacement thickness ($\overline{\delta}^*_x$) decreases but the enthalpy thickness ($\overline{\delta}_{H_x}$) increases. The reason behind this is that when we increase rotation of the sphere, the flow in the meridional direction gets reduced considerably in the boundary layer whereas it helps to increase the azimuthal flow. On the other hand, due to increase in rotation, the flow interaction in the boundary layer increases which helps in enhancing the enthalpy thickness ($\overline{\delta}_{H_x}$). An increase in the magnetic field strength (M) causes reduction in enthalpy thickness whereas it increases the displacement thickness. The boundary layer displacement thickness ($\overline{\delta}^*_x$) becomes negative for cases of favourable pressure gradient with very low wall enthalpy (temperature). This occurs because the surface cooling produces an increase in density near the wall, so that there is more mass flow per unit flow area within the boundary layer than in the external flow [14]. However, such results are not shown here.

Figure 5 shows the effect of rotation (λ) and time (t^*) on the growth of velocity and enthalpy distribution (F, s, g). The cause of unsteadiness is the same as that described in Fig. 3. It is observed that the meridional velocity (F) shows overshoot for high rotation ($\lambda = 10$) and with time, when an impulsive decrease in the wall enthalpy is considered, whereas impulsively increasing wall enthalpy process does not show any overshoot for $t^* > 0.1$, but it shows oscillatory nature in the new steady state ($t^* = 2$). The meridional velocity is especially affected by compressibility. When the wall is heated, the density within certain layers of the boundary layer is reduced significantly, in spite of viscous retardation, the local flow is accelerated more than the external flow. Then velocity (F) in some portion of the boundary layer reaches a maximum value greater than 1.0 before returning to its final value 1.0. The phenomenon can occur even when the wall temperature is less than the recovery temperature [14]. Here an increase in rotation has the effect of increasing the excess of the local velocities over the external velocity. Another interesting observation from Fig. 5 is that both meridional and azimuthal velocity ($F \& s$) overshoot temporarily the eventual steady state value when an impulsive increase in the wall enthalpy is considered, whereas in the impulsive decreasing process they increase with time and finally reach a new steady state. The enthalpy profiles (g) show that at each point inside the boundary layer, enthalpy increases or decreases with time while approaching a new steady state, depending on the situation whether an impulsive increase or decrease of wall enthalpy is considered. It may also be observed that the enthalpy thickness increases when an impulsive increase in wall enthalpy is considered.

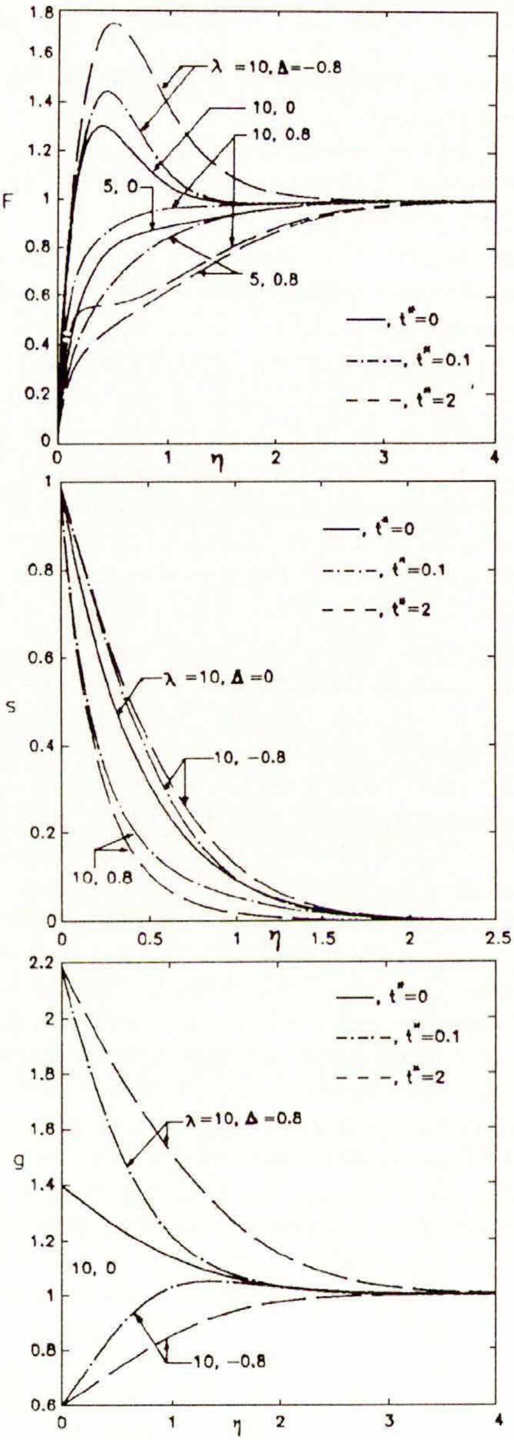

FIG. 5. Effects of rotation (λ) and time (t^*) on the velocity and enthalpy (F, s, g) profiles for $M = 5$, $f_w = 0.0$, $g_w = 1.4$ and $\omega = 0.5$; (unsteadiness due to impulsive change in wall enthalpy).

CASE 2. In this case unsteadiness is caused by a sudden change in rotation of the sphere

Here we describe the transient motion when an impulsive change is given to the angular rotation of the sphere placed in a uniform axial stream of electrically conducting fluid.

Figure 6 shows the variation of skin friction and heat transfer $[\overline{C}_{f_x}, -\overline{C}_{f_y}, \overline{\mathrm{St}}]$ with time, and the effects of wall enthalpy (g_w) and the viscosity index (ω) on the above mentioned quantities when the angular rotation of the sphere is suddenly changed to a new constant value. As it can be observed from the inset of Fig. 6, showing the effect of impulse immediately after it is imparted, the azimuthal skin friction $[-\overline{C}_{f_y}]$ suffers much change in the beginning $(t^* = 0+)$. It increases or decreases to a maximum or minimum value from the initial $(t^* = 0)$ steady state and then decreases or increases with time (depending on whether impulsive increase or decrease in rotation is considered) while approaching a new steady state in an asymptotic way. This is due to the fact that the rotation is considered along the azimuthal direction and an impulsive change in the rotation of the sphere causes an instantaneous steep change in the azimuthal shear at the surface of the sphere. The transition for meridional skin friction and heat transfer $(\overline{C}_{f_x} \& \overline{\mathrm{St}})$ is observed to be smooth. It may also be observed that it is the azimuthal skin friction $[-\overline{C}_{f_y}]$ which reaches the new steady state faster, whereas the heat transfer takes more time to settle down. Moreover, once again it is observed that the transition time for impulsive decay process is longer than the impulsive increasing process as observed in Case 1. Figure 6 also shows that as wall enthalpy (g_w) increases, both meridional skin friction and heat transfer $(\overline{C}_{f_x}, \overline{\mathrm{St}})$ decrease, whereas the azimuthal skin friction $[-\overline{C}_{f_y}]$ shows the opposite effect. The effect of variation of the density-viscosity product across the boundary layer is characterized by the parameter ω. Both skin friction and heat transfer are found to increase significantly as the viscosity-index ω increases, however results are shown only for meridional skin friction for the sake of brevity.

Figure 7 shows the distribution of velocity field $[F, s]$ with time and the effect of magnetic parameter M on them. The meridional velocity (F) shows overshoot when an impulsive increase in rotation is considered. An interesting observation is that the meridional velocity oscillates within the boundary layer (for impulsive increase in rotation), but does not show any overshoot, when magnetic field strength (M) is increased, whereas the rest of the profiles approach their free stream value in a monotonic fashion. It may also be observed that the azimuthal velocity (s) reaches its new steady state faster $(t^* = 0.1)$ when the impulsive increase in rotation is considered, whereas it takes longer time to settle down when the rotation of the sphere is reduced impulsively. In the case of impulsive decrease in rotation, both the velocities $(F \& s)$ overshoot temporarily the eventual or new steady state value.

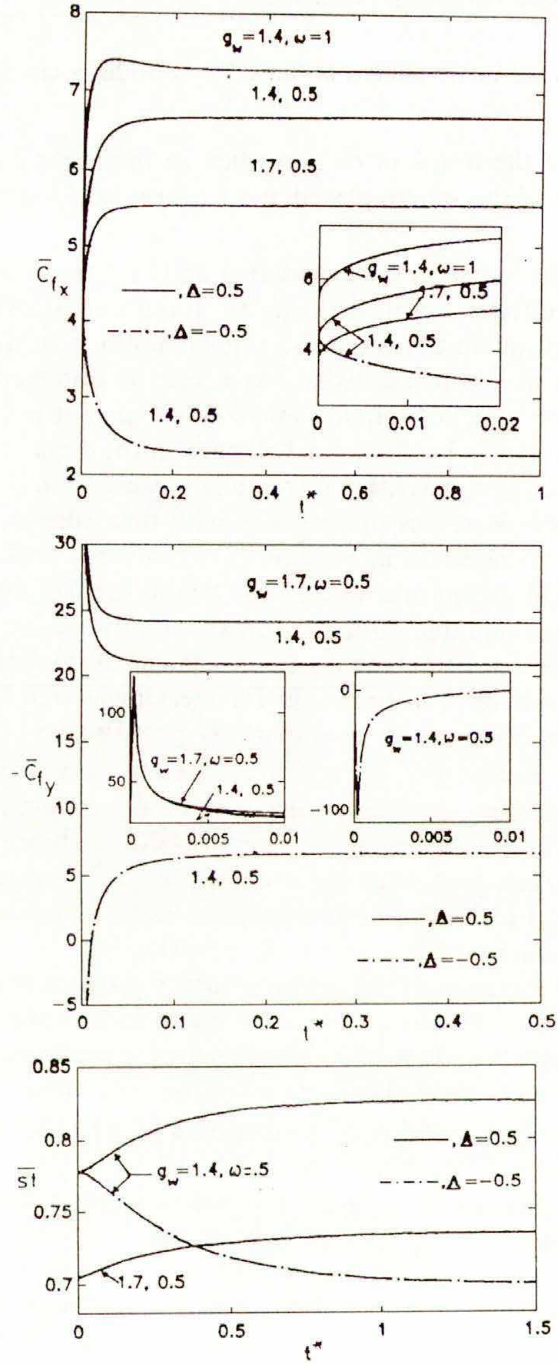

FIG. 6. Effects of wall enthalpy (g_w) and viscosity-index (ω) on skin frictions and heat transfer ($\overline{C}_{fx}, -\overline{C}_{fy}, \overline{\mathrm{St}}$) for $f_w = 0$, $M = 5$ and $\lambda = 6$; (unsteadiness due to impulsive change in rotation).

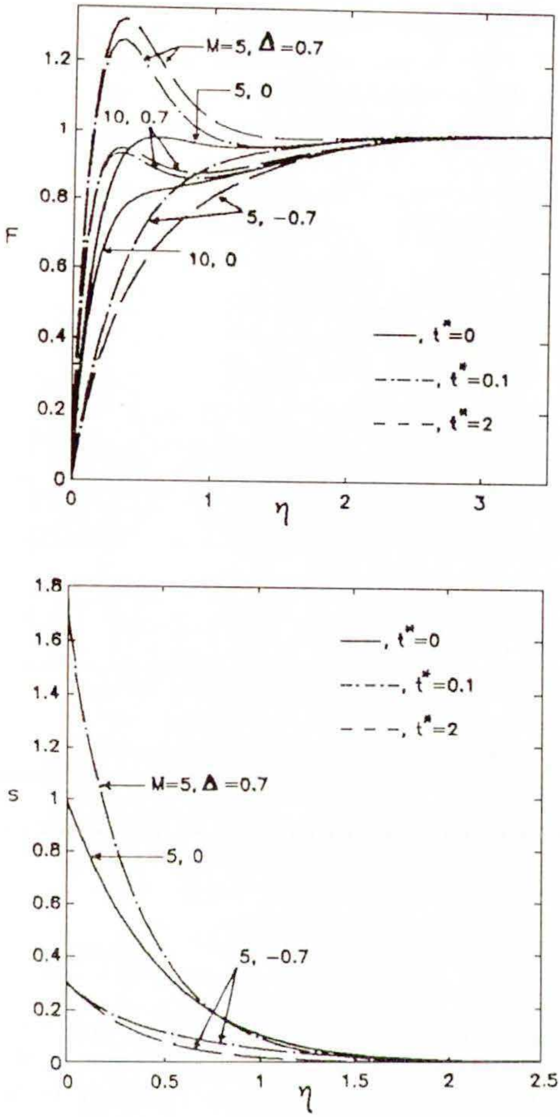

FIG. 7. Effects of magnetic parameter (M) and time (t^*) on the velocity (F, s) profiles for $f_w = 0$, $g_w = 1.4$, $\lambda = 7$ and $\omega = 0.5$; (unsteadiness due to impulsive change in rotation).

CASE 3. Unsteadiness caused by sudden change in the meridional free-stream velocity

Figure 8 shows the distribution of meridional velocity (F) when its free stream value is changed impulsively. The velocities overshoot inside the boundary layer before approaching their free stream value. The new steady ($t^* = 2$) profile shows its oscillatory nature when the impulsive decrease in the free stream is considered. Moreover, it has been observed that at time $t^* = 0.1$ its (F) value at any point inside the boundary layer is higher than the profile in its new steady state ($t^* = 2$). The situation is just reverse when an impulsive increase in the free stream is considered. The unsteady profiles ($t^* > 0$) show its monotonic nature at the edge of the boundary layer; this is probably because the impulse is given at the free stream.

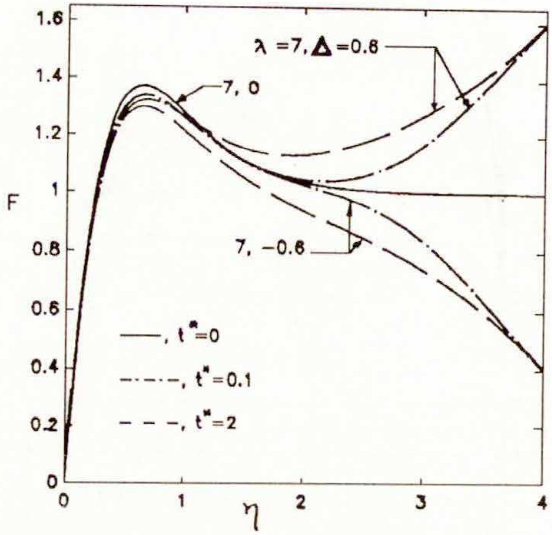

FIG. 8. The velocity (F) profiles for $f_w = 0$, $M = 5$, $g_w = 1.4$, $\lambda = 7$ and $\omega = 0.5$; (unsteadiness due to impulsive change in the meridional free stream velocity).

5. Conclusions

The transient behaviour of flow and heat transfer over a rotating sphere has been investigated numerically due to impulsive changes in the flow physics. A large change in the flow is observed at the early stage of transient motion. The rotation increases friction, heat transfer at the surface and the enthalpy thickness. The meridional velocity (F) shows overshoot for high rotation and for the impulsive reduction of the wall enthalpy. It oscillates inside the boundary layer for higher magnetic field strength when an impulsive increase in rotation is considered. The transition time is longer for impulsive reduction processes, compared to impulsive increasing processes. Heat transfer takes longer time to settle down than skin frictions. For both impulsive increase in wall enthalpy and impulsive decrease in rotation of the sphere, the velocities overshoot temporarily before getting settled to the eventual steady state value, whereas, for the impulsive decrease in wall enthalpy or for the impulsive increase in rotation, the velocities increase with time while approaching a new steady state.

References

1. E. BOLTZE, *Grenzschichten und Rotationskörpern in Flüssigkeiten mit kleiner Reibung. Thesis*, Göttingen 1908.
2. S.C.R. DENNIS and J.D.A. WALKER, *The initial flow past an impulsively started sphere at high Reynolds number*, J. Engng. Math., **5**, 263–278, 1971.
3. S.C.R. DENNIS and J.D.A. WALKER, *Numerical solution for time-dependent flow past an impulsively started sphere*, Phys. Fluids, **15**, 517–525, 1972.
4. W.H.H. BANKS and M.B. ZATUSKA, *The collision of unsteady laminar boundary layers*, J. Engng. Math., **13**, 193–212, 1979.
5. T. CEBECI, K. STEWARTSON and S.M. SCHIMKE, *Unsteady boundary layers close to the stagnation region of slender bodies*, J. Fluid Mech., **147**, 315–332, 1984.
6. S.C.R. DENNIS and P.W. DUCK, *Unsteady flow due to an impulsively started rotating sphere*, Computers Fluids, **16**, 291–310, 1988.
7. P.W. DUCK, *The unsteady laminar boundary layer on an axisymmetric body subject to small amplitude fluctuation in the free stream velocity*, J. Fluid Mech., **232**, 415–438, 1991.
8. M.C. ECE, *The initial boundary layer flow past a translating and spinning rotational symmetric body*, J. Engng. Math., **26**, 415–428, 1992.
9. M. KUMARI and G. NATH, *Heat and mass transfer in unsteady compressible axisymmetric stagnation point boundary layer flow over a rotating body*, Int. J. Heat Mass Transfer, **25**, 290–293, 1982.
10. C.S. VIMALA and G. NATH, *Unsteady laminar boundary layers in a compressible stagnation flow*, J. Fluid Mech., **70**, 561–572, 1975.
11. H. SCHLICHTING, *Boundary layer theory*, McGraw-Hill, New York 1979.
12. K.R. CRAMER and S.I. PAI, *Magneto-fluid dynamics for engineers and applied physics*, McGraw-Hill, New York 1973.
13. W.L. BADE, *Stagnation point heat transfer in a high temperature inert gas*, Phys. Fluids, **5**, 150–154, 1962.
14. C.B. COHEN and E. RESHOTKO, *Similar solutions for the compressible laminar boundary layer with heat transfer and pressure gradient*, NACA TN, 1293, 1956.

DEPARTMENT OF MATHEMATICS
INDIAN INSTITUTE OF SCIENCE, BANGALORE, INDIA.

Received July 30, 1996.